Chapter 6
Threshold Control for Stabilization of Unstable Periodic Orbits in Chaotic Hybrid Systems

Daisuke Ito, Tetsushi Ueta, Takuji Kousaka, Jun-ichi Imura and Kazuyuki Aihara

6.1 Introduction

Various deterministic dynamical systems including nonlinear electric circuits show chaotic phenomena characterized by the sensitivity to small perturbations, positive Lyapunov exponents, and their complex orbit structure. It is well known that an infinite number of unstable periodic orbits (UPOs)are embedded in a chaotic attractor [1].

Based on the Poincaré mapping, a UPO in a continuous-time system can be expressed as an unstable periodic point (UPP) in the corresponding discrete-time system. The Ott-Grebogi-Yorke (OGY) method was the pioneering attempt to stabilize UPPs [2] by pushing the orbit near the stable manifold of the target UPP with very

D. Ito (✉)
Advanced Technology and Science, System Innovation Engineering,
Tokushima University, 2-1 Minamijyousanjima, Tokushima 770-8504, Japan
e-mail: d-ito@is.tokushima-u.ac.jp

T. Ueta
Center for Administration of Information Technology, Tokushima University,
2-1 Minamijyousanjima, Tokushima 770-8506, Japan
e-mail: ueta@tokushima-u.ac.jp

T. Kousaka
Faculty of Engineering, Oita University, 700 Dannoharu, Oita 870-1192, Japan
e-mail: takuji@oita-u.ac.jp

J. Imura
Graduate School of Information Science and Engineering, Tokyo Institute of Technology,
2-12-1 O-Okayama, Meguro, Tokyo 152-8552, Japan
e-mail: imura@mei.titech.ac.jp

K. Aihara
Institute of Industrial Science, The University of Tokyo, 4-6-1 Komaba, Meguro,
Tokyo 153-8505, Japan
e-mail: aihara@sat.t.u-tokyo.ac.jp

K. Aihara et al. (eds.), *Analysis and Control of Complex Dynamical Systems*,
Mathematics for Industry 7, DOI 10.1007/978-4-431-55013-6_6

small parameter perturbations. If it fails, a retry in near future is expected because of the recurrence property of the chaos, i.e., the uncontrolled orbit will comes close to the target UPP again. With this recurrence, there is a possibility that stabilizing the target UPP with a tiny control input, which is proposed to the distance between the current state and the UPP. In the very small area around the target UPP, this kind of problems can be considered by linear control theory. The controlling chaos by the pole assignment method has been proposed [3]. The feedback gain of this controller can be designed with assigned poles regarding the characteristic equation for the variational equation [4, 5]. Extensions of the methods are applied to chaotic hybrid systems [6]. In these conventional methods, the amplitude of the control input is basically proportional to the error between the current state of the orbit and the UPP. As mentioned above, the recurrence property of chaotic dynamics realizes that the orbit will visit a neighborhood of the UPP in future, thus the control input can be small at that moment.

Other nonlinear control schemes including the delayed feedback control [7] and its extensions [8, 9] have been proposed. Related methods such as external force control [10], and occasional proportional feedback [11–16] are also discussed from a practical view point.

In these methods, the control input is basically added to the state or parameters of the system. Thus the controller must vary these values which may be difficult to change; e.g., in electrical circuits, the controller requires to change the amount of a resistor or a capacitor quickly.

While, hybrid systems has been intensively studied for a decade [17]. In those systems, a flow described by differential equations is interrupted by the discrete events, and then an impulsive jumping or a switching of the governing differential equations happens. Thus the flow may changes non-smoothly, and it may cause peculiar bifurcations [18]; e.g., in chaotic spiking oscillators [19], state-dependent switching generates two different flows where a bifurcation phenomena and a chaotic response are guaranteed theoretically. In general, the switching mechanism is not explicitly described in the differential equations, but it affects certainly dynamical behavior of the system [20, 21]. In electric circuits, a variable threshold is realized by an analog switch (multiplexer); therefore, to choose the threshold value as a control input is reasonable.

For a specific hybrid system, the controlling chaos based on the linear control theory can be realized by applying the Poincaré section on the border [6]. UPPs in the derived discrete-time system are controlled with the same framework of the conventional control method, i.e., the control input is added into a system parameter or the state as a small perturbation successively. In other words, the whole control system spends a certain amount of energy until the control scheme completes the stabilization.

A threshold value in the given hybrid system is not used as the control parameter because dynamical affection with perturbed threshold values has not been evaluated yet. In the previous study [20] we clarified the derivatives and variational equations of the given hybrid systems about threshold values. Thereby we apply these results

to controlling chaos; namely, we try to design a control scheme with variations of threshold values theoretically.

Now let us restate our purpose in this chapter. We stabilize a UPO embedded within a chaotic attractor in a hybrid system by varying its threshold values. The control system compares the current state variable with the threshold value, and updates the threshold value instantly and slightly. The orbit starting from the current Poincaré section (the threshold value) does not receive any control until it reaches the next section. Although Murali and Sinha [22] have proposed a chaos controller by featuring the perturbation of attached threshold values, the objective system is not a hybrid system and the proposed controller stabilizes UPOs by clipping the voltage of a system with a simple circuit. Parameter values of the controller are provided by trial and error. In our method, the control vector is computed systematically by applying the linear control theory. We demonstrate control results of a 1D switching chaotic system and a 2D chaotic neuron, and evaluate its control performances as the controller by specifying basins of attraction. Moreover, a related experiment is given for the former system.

6.2 Design of Controller with Perturbation of the Threshold Value

Let us consider the n-dimensional and m-tuple differential equations described by

$$\frac{dx}{dt} = f_i(x),\ i = 0,\ 1,\ \ldots,\ m-1, \tag{6.1}$$

where $t \in \mathbb{R}$ is time, $x \in \mathbb{R}^n$ is the state and $f_i : \mathbb{R}^n \to \mathbb{R}^n$ is a C^∞ class function.

Suppose that Π_i is a transversal section to the orbit and set $x_0 = x(0) \in \Pi_0$, then the solution of (6.1) is given by

$$x(t) = \varphi(x_0, t).$$

Now we provide Π_i with a threshold value as follows:

$$\Pi_i = \left\{ x \in \mathbb{R}^n \,|\, q_i(x,\ \theta_i) = 0 \right\},$$

where q_i is a differentiable scalar function, and θ_i is a unique parameter that defines the position of Π_i. Note that Π_i becomes also a local section, and θ_i is independent from the vector field in (6.1). When an orbit governed by f_i reaches the section Π_i, the governing function is changed to f_{i+1}. If the orbit passing through several sections reaches Π_0 again, then m local maps are defined as follows:

$$\begin{aligned} T_0 &: \Pi_0 \to \Pi_1, \\ &\quad x_0 \mapsto x_1 = \varphi_0(x_0,\ \tau_0), \\ T_1 &: \Pi_1 \to \Pi_2, \\ &\quad x_1 \mapsto x_2 = \varphi_1(x_1,\ \tau_1), \\ &\quad \vdots \\ T_{m-1} &: \Pi_{m-1} \to \Pi_0, \\ &\quad x_{m-1} \mapsto x_0 = \varphi_{m-1}(x_{m-1},\ \tau_{m-1}), \end{aligned} \tag{6.2}$$

where τ_i is the passage time from Π_i to Π_{i+1}, and depends on the state x_i and the parameter θ_{i+1} of the local section Π_{i+1}. Assume that $y(k) \in \Sigma \subset \mathbb{R}^{n-1}$ is a location on local coordinates, then there is the projection satisfying $\eta(x(k)) = y(k)$. Let the composite map of $T_i,\ i = 0,\ 1, \ldots, m-1$ be the solution starting in $\eta^{-1}(y(0)) = x(0) \in \Pi_0$. From (6.2), the Poincaré map T is given by the following composite map:

$$T(y(k),\ \theta_0,\ \theta_1,\ \ldots,\ \theta_{m-1}) = \eta \circ T_{m-1} \circ \cdots \circ T_1 \circ T_0 \circ \eta^{-1}.$$

Thus

$$y(k+1) = T(y(k),\ \theta_0,\ \theta_1,\ \ldots,\ \theta_{m-1}).$$

When the orbit starting from $x_0 \in \Pi_0$ returns x_0 itself, this orbit forms a periodic orbit and it is defined as the fixed point by using the Poincaré map T as follows:

$$y_0 = T(y_0,\ \theta_0,\ \ldots,\ \theta_{m-1}).$$

The corresponding characteristic equation is given by

$$\chi(\mu) = \det\left(\frac{\partial T(y_0)}{\partial y_0} - \mu I\right) = 0.$$

To apply the pole assignment method, the derivatives of the Poincaré map are required to compute a control gain [3]. The equations in (6.2) are, in fact, differentiable with respect to the state, thus each derivative is given as follows:

$$\begin{aligned} \frac{\partial T_i}{\partial x_i} &= \left[I - \frac{1}{\dfrac{\partial q_{i+1}}{\partial x}\dfrac{\partial \varphi_i}{\partial t}} \frac{\partial q_{i+1}}{\partial \theta_{i+1}} \frac{\partial \varphi_i}{\partial t} \right] \frac{\partial \varphi_i}{\partial x_i}, \\ \frac{\partial T}{\partial y_0} &= \frac{\partial \eta}{\partial x} \left(\prod_{i=1}^{m} \frac{\partial T_{m-i}}{\partial x_{m-i}} \right) \frac{\partial \eta^{-1}}{\partial y}, \end{aligned} \tag{6.3}$$

$$\frac{\partial T_{j-1}}{\partial \theta_j} = \frac{-1}{\dfrac{\partial q_j}{\partial x}\dfrac{\partial \varphi_{j-1}}{\partial t}} \frac{\partial q_j}{\partial \theta_j}\frac{\partial \varphi_{j-1}}{\partial t},$$

$$\frac{\partial T}{\partial \theta_j} = \frac{\partial \eta}{\partial x}\prod_{i=1}^{m-j}\frac{\partial T_{m-i}}{\partial x_{m-i}}\frac{\partial T_{j-1}}{\partial \theta_j}. \tag{6.4}$$

We can suppose here that $(\partial q_{i+1}/\partial x) \times (\partial \varphi_i/\partial t)$ and $(\partial q_j/\partial x) \times (\partial \varphi_{j-1}/\partial t)$ are non-zero unless the orbit and sections are crossed tangentially.

Suppose that $\xi(k)$ is a small perturbation and $u(k)$ is intended to be a control input defined later. When the parameter θ_j is chosen as a controlling parameter, the variational equations around the fixed point are expressed as

$$y(k) = y^* + \xi(k),\ \theta_j(k) = \theta_j + u(k). \tag{6.5}$$

After one iteration of T, we have

$$\begin{aligned} y(k+1) &= T(y^* + \xi(k),\ \theta_j + u(k)) \\ &\approx y^* + \frac{\partial T}{\partial y^*}\xi(k) + \frac{\partial T}{\partial \theta_j}u(k). \end{aligned}$$

Therefore we obtain the difference equation defined by the derivative of T as follows:

$$\xi(k+1) = D_{y^*}\xi(k) + D_{\theta_j}u(k), \tag{6.6}$$

where $D_{y^*} = \partial T/\partial y^*$ and $D_{\theta_j} = \partial T/\partial \theta_j$. Note that (6.6) holds when the state $y(k)$ is located to be adjacent to the fixed point y^*.

To stabilize $\xi(k)$ at the origin, a state feedback control is designed as follows [5]:

$$u(k) = K^{\mathsf{T}}\xi(k), \tag{6.7}$$

where T is a transpose and K is an appropriate $n-1$ dimensional vector designed by the pole assignment method. Thus we have

$$\xi(k+1) = [D_{y^*} + D_{\theta_j}K^{\mathsf{T}}]\xi(k). \tag{6.8}$$

The corresponding characteristic equation is given by

$$\chi(\mu) = \det(D_{y^*} + D_{\theta_j}K^{\mathsf{T}} - \mu I) = 0. \tag{6.9}$$

The stability condition at the origin is $|\mu_i| < 1,\ i = 1,\ 2,\ \ldots,\ n-1$.

In the conventional chaos control methods, a control input is applied into the specific system parameter as a small perturbation. During a transition state, the control system consumes certain control energy given by integration of such perturbations even if small. Thus $\varepsilon = \int_0^\infty ||u(t)||dt$ is regarded as controlling energy.

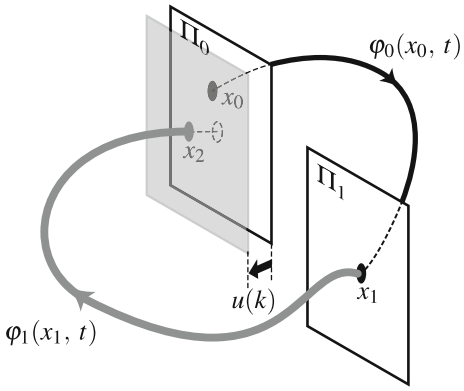

Fig. 6.1 Relationship between the flow and sections. Our method adjusts the position of the local section Π_0 only. The state and vector fields are not affected by the control input

In our method, the control input $u(k)$ is added into θ_j; see (6.5). Figure 6.1 depicts a schematic diagram of the method. The location of the section Π_0 defined by θ_0 is shifted by $u(k)$ instantly when the orbit $\varphi_0(t,\ x_0)$ departs from Π_0. No actual control input is added into the system. The state-feedback is utilized only to determine the dynamic threshold value, thus the orbit starting from the current threshold value reaches the next controlled threshold value without any control energy.

It is noteworthy that this is an energy-saving control scheme. For example, let us suppose that we want to put a ball into a bucket with bouncing once on the wall. In Fig. 6.2a, an electrical fan modifies the trajectory of the ball by blowing against it. The fan consumes electrical energy continuously during transient. The conventional methods look like this situation. On the other hand, changing the position of the wall

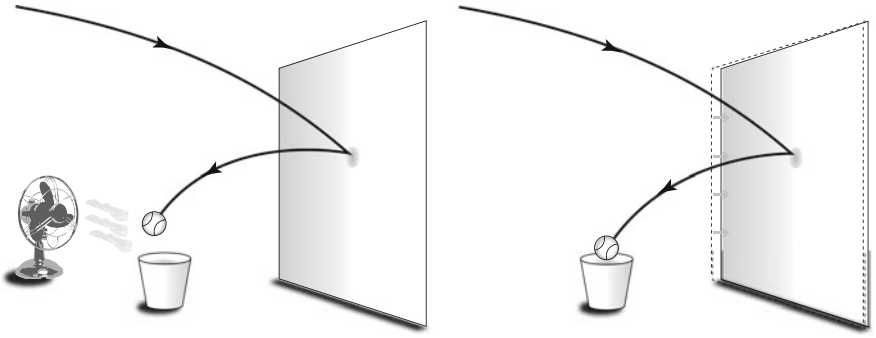

Fig. 6.2 Concepts of controlling schemes. In a conventional method, a controller, e.g. an electrical fan, has to blow the ball to put it to the bucket. Therefore, it requires a powerful controller to move a ball. In the case to use the threshold value as a perturbation parameter, the controller only move the position of a wall or a goal, and does not influence the ball directly

also provides the same effect with (a), i.e., the original position of the wall may cause failure of the shoot, but a desirable trajectory can be realized by letting the wall to be in a proper position, see Fig. 6.2b. Realistically, not a little effort is required to move the wall compared with a short-time operation of the fan, however, in the electric circuit, such movement of the wall is easily realized, e.g., by a change of the value of the threshold for an operational amplifier. Note that no control energy consumed during this scheme. Only small energy is required when the old threshold value is updated. The orbit runs without any control until it reaches the next threshold value.

6.3 A Simple Chaotic System

Let us consider a simple interrupt chaotic system [23] shown in Fig. 6.3 as an example. The switch is flipped by a certain rule depending on the state and the period. Assume that v is the state variable, and then the normalized equation is given as follows:

$$\dot{v} = -v + E,$$
$$\text{if} \quad t = n\rho \quad \text{then} \quad E \leftarrow E_1, \quad \text{if} \quad v > E_r \quad \text{then} \quad E \leftarrow 0$$

where $n \in \mathbb{N}$, E_1 and E_r are a direct voltage bias and a switching threshold value, respectively. ρ is the period of the clock pulse input. Figure 6.4 illustrates the dynamical behavior. If the Poincaré section is defined as $\Pi = \{v \in \mathbb{R};\ t = n\rho\}$, trajectories stroke two types of solutions (Fig. 6.5), and they can be solved exactly, see, [24]. Therefore the system can be discretized by the Poincaré section, and redefined as follows:

$$v'(k+1) = g(v'(k)) = \begin{cases} (v'(k) - E_1)e^{-\rho} + E_1, & \text{if} \quad v'(k) < d, \\ E_r \dfrac{v'(k) - E_1}{E_r - E_1} e^{-\rho}, & \text{otherwise}, \end{cases} \tag{6.10}$$
$$d = (E_r - E_1)e^{\rho} + E_1.$$

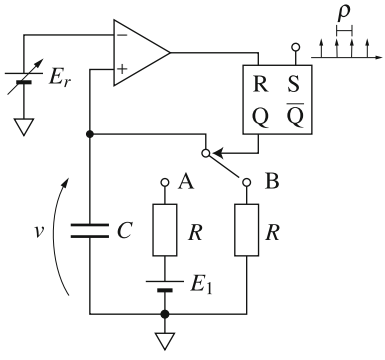

Fig. 6.3 Circuit model of an interrupt chaotic system. ρ and E_r represent the period of the clock pulse input and the switching threshold value, respectively

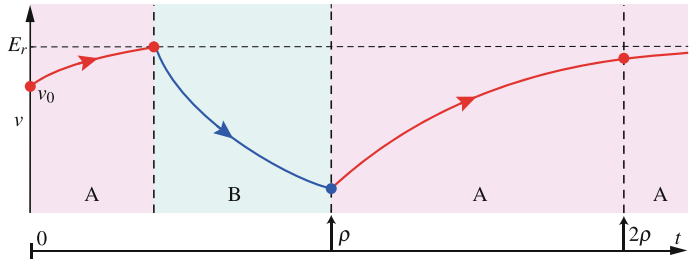

Fig. 6.4 The switching behavior. When the capacitor voltage reaches to the threshold value E_r, the switch is flipped to the position B. If the time t is ρ, the switch is flipped to the position A

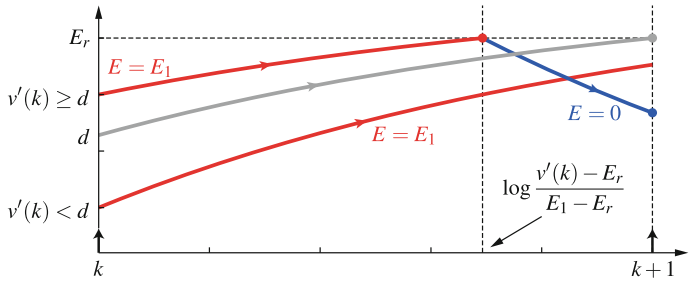

Fig. 6.5 The sketch of a simple chaotic interrupt system. There are two types of trajectories depending on the initial value $v'(k)$. If $v'(k)$ is less than d, the trajectory reaches $v'(k+1)$ without interruption. Otherwise, the trajectory reaches the threshold value E_r, and E is changed to zero

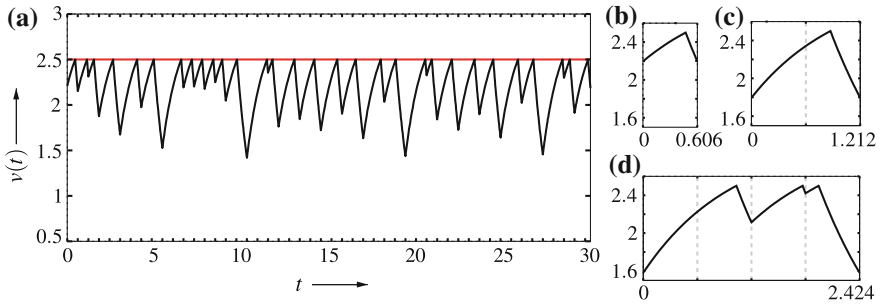

Fig. 6.6 **a** A sample trajectories of a chaotic attractor with $E_1 = 3$, and $E_r = 2.5$. **b**, **c**, and **d**: Period 1, 2 and 4 UPOs embedded in the chaos, respectively

Note that $v'(k) = v(k\rho)$. The solution ψ is defined by (6.11):

$$\psi(v'(0), k) = v'(k), \ \psi(v'(0), 0) = v'(0) = v(0). \tag{6.11}$$

A chaotic attractor and three UPOs with parameters $E_1 = 3$, $E_r = 2.5$ and $\rho = 0.606$ are shown in Fig. 6.6. Table 6.1 lists the periods, states and multipliers of some UPOs. Each orbit is confirmed to be a UPO.

Table 6.1 Periods, states, and multipliers of UPOs in Fig. 6.6b–d

Attractor	Period	v^*	μ
(b) UPO_1	1	2.195202	−2.727643125796
(c) UPO_2	2	1.794216	−1.488007404341
		2.34221	
(d) UPO_4	4	1.580281	−11.070830176867
		2.225503	
		2.112552	
		2.420642	

From Eqs. (6.8) and (6.9), we can choose the control gain as

$$K = \frac{q - D_{v^*}}{D_{E_r}},$$

where $D_{v^*} = \partial T/\partial v^*$ and $D_{E_r} = \partial T/\partial E_r$ are derivatives of T, and can be calculated as follows:

$$\frac{\partial T}{\partial v^*} = \frac{\partial \psi}{\partial v^*}(v^*,\ p),\ \frac{\partial \psi}{\partial v^*}(v^*,\ k+1) = \left.\frac{\partial g}{\partial v'}\right|_{v'=v'(i)} \frac{\partial \psi}{\partial v^*}(v^*,\ k),$$
$$\frac{\partial \psi}{\partial v^*}(v^*,\ 0) = I, \tag{6.12}$$

$$\frac{\partial T}{\partial E_r} = \frac{\partial \psi}{\partial E_r}(v^*,\ p),\ \frac{\partial \psi}{\partial E_r}(v^*,\ k+1) = \left.\frac{\partial g}{\partial v'}\right|_{v'=v'(i)} \frac{\partial \psi}{\partial v^*}(v^*,\ k) + \left.\frac{\partial g}{\partial E_r}\right|_{v'=v'(i)},$$
$$\frac{\partial \psi}{\partial E_r}(v^*,\ 0) = 0, \tag{6.13}$$

where the symbol $p \in \mathbb{N}^+$ is the period of the target trajectory, and q is a desirable pole for the controlling, and $|q| < 1$ is required for stabilization. When the clock pulse is input at $t = k\rho$, $u(t)$ is generated as $K(v^* - v'(k))$ from (6.7), and it is added to the switching threshold E_r. Figure 6.7 shows the behavior of $u(t)$ and the system. When $u(t)$ is applied to the system, the threshold value is changed, and the behavior of the system is controlled.

6.3.1 Numerical Simulation

We show some results of the chaos control by referring to Fig. 6.8, where each graph shows a transition response of the orbit and the threshold value. From this figure, we confirm that each UPO is controlled to become a stable periodic orbit by several

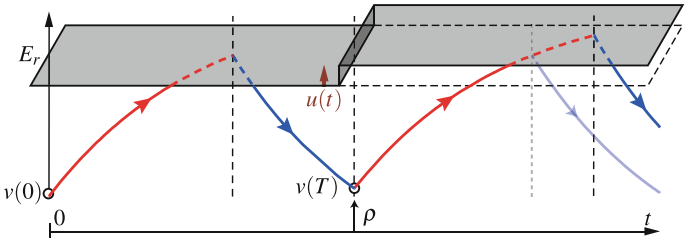

Fig. 6.7 Controller affects the switching threshold E_r, thus the control input $u(t)$ biases E_r. By doing this, the controller can control the trajectory without any effect on the dynamical equations and vector fields

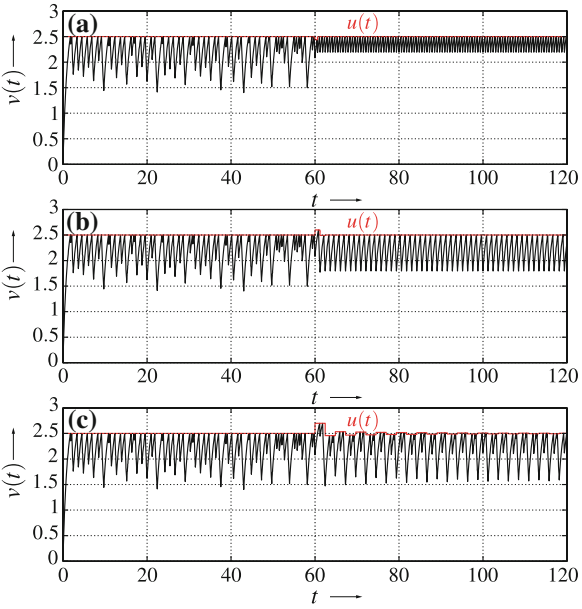

Fig. 6.8 Transition responses of controlled UPOs and the threshold values. **a** Period-1, **b** period-2 and **c** period-4 solutions shown in Table 6.1 are stabilized. Note that $u(t)$ does not affect the state and vector fields directly

renewals of $u(t)$. The UPO_4 in Fig. 6.8c has a longer renewal span than other UPOs because a renewal span depends on the period of the target UPO.

Figure 6.9 shows basins of attraction of UPOs with our controller in the q-$v(0)$ plane. White regions in the figure indicate the initial values in which the UPO could be stabilized, and black regions indicate failure of the controlling. This shows that all UPOs could be stabilized easily with relatively small initial values. Additionally, UPOs can also be stabilized at a negative initial value. However, in larger initial values, the UPO_4 could not be controlled. The pole assignment method renews the control signal on a periodic basis only. Therefore, this technique is less effective for long-period UPOs such as the UPO_4.

Figure 6.6a reveals that the chaotic attractor wanders within $1.3 < v(t) < 2.5$. The basin of attraction in this range is shown by white regions in Fig. 6.9. Thus the

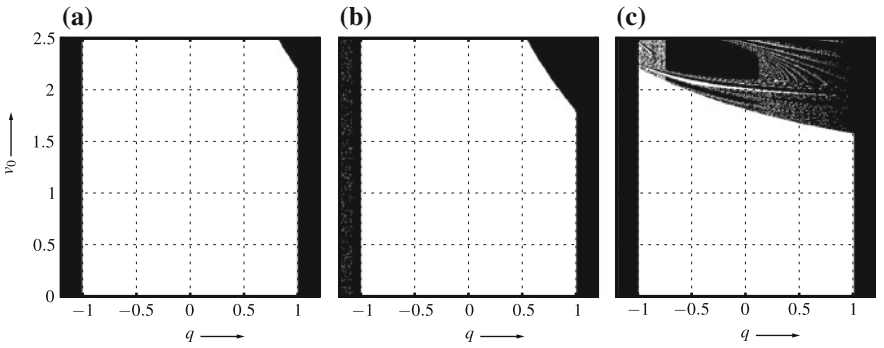

Fig. 6.9 Basins of attraction resulting from a control experiment. (*White* stabilizable regions and *black* unstabilizable regions.) The *horizontal* and *vertical axes* are the parameter q of the controller and the initial state of the system, respectively

UPO_1 and the UPO_2 are stabilized robustly. The threshold control performs well for this simple chaotic system.

6.3.2 Circuit Implementation

Owing to the sample holder synchronized with a clock pulse, our controller is very easy to implement, thus we show the circuit implementation and experimental results.

Figure 6.10 shows the circuit diagram of the system and the controller. The subtractor and the inverter 1 generate $u(t)$, and the adder and the inverter 2 add the control input to the switching threshold. The switching threshold generated by this controller is applied to the system as a perturbation of the reference value E_r.

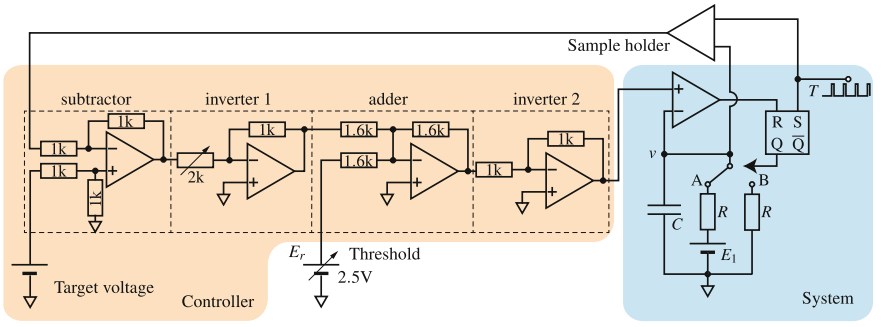

Fig. 6.10 Circuit diagram of a simple chaotic system and the proposed controller. The controller is composed of four parts. The variable resistance defines the controlling gain, and the voltage source is the target voltage v^*

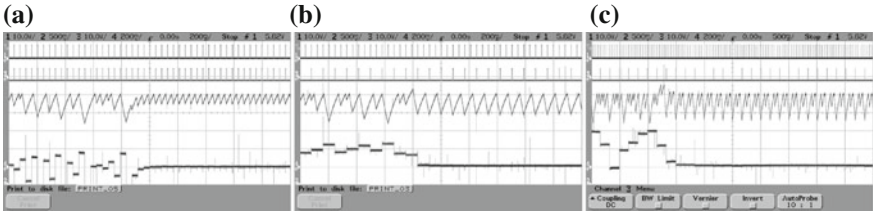

Fig. 6.11 Results of the laboratory experiments. **a** UPO_1, **b** UPO_2, and **c** UPO_4. (*For each shot*: *Top row* the clock pulse input, *2nd row* the timing of the renewal of the controlling signal, *3rd row* the voltage of the capacitor [10V/DIV], and the *bottom* the control input voltage [200mV/DIV]. The *horizontal axis* time [(**a**, **b**) 200 and (**c**) 500 ms/DIV].) The controlling started at 800 ms. The circuit is quickly converged to each periodic orbit after the control transition

We use ICs TC4053BP and LM325M as the logic switch and the comparator in this experiment.

Figure 6.11 shows a transition response of the circuit experiment. In these figures, the top, 2nd, 3rd and bottom time series show the clock pulse input, the timing of the renewal of the control signal, the voltage of the capacitor as the orbit v and the control signal, respectively. It is confirmed that control inputs converged to zero, and orbits are certainly stabilized at UPOs.

6.4 Izhikevich Model

Let us consider the Izhikevich model [25] as the second example. As is well known that this model is two dimensional, and behaves chaotically in certain parameter setting [26]. The equations are given as follows:

$$\dot{z}(t) = \begin{pmatrix} 0.04v + 5v + 140 - w + I \\ a(bv - w) \end{pmatrix},$$

$$\text{if} \quad v = \theta, \quad \text{then} \quad v \leftarrow c, \quad w \leftarrow w + d,$$

where $z = (v,\ w)$ is the state, and I, a, b, c, d and θ are parameters. Especially, c and d show the jumping dynamics, and θ defines the threshold value of the jumping. Figure 6.12 illustrates the dynamical behavior.

A chaotic attractor and three UPOs that are involved in it with parameters $a = 0.2$, $b = 2$, $c = -56$, $d = -16$, $I = -99$ and $\theta = 30$ are shown in Fig. 6.13. Table 6.2 lists the periods, states and multipliers of several UPOs. Each orbit is confirmed to be a UPO.

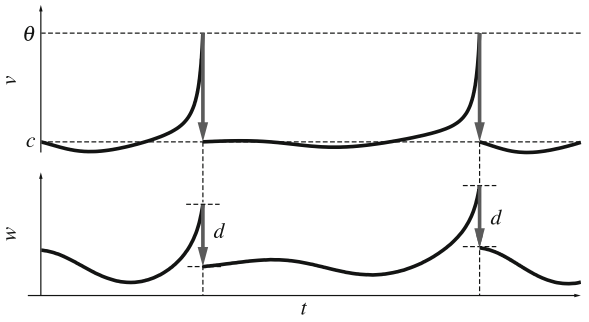

Fig. 6.12 The sketch of the typical behavior of the Izhikevich model. If the state $z(t)$ reaches the threshold value θ, the state $z(t) = (\theta,\ w(t))$ jumps to $z(t) = (c,\ w(t) + d)$

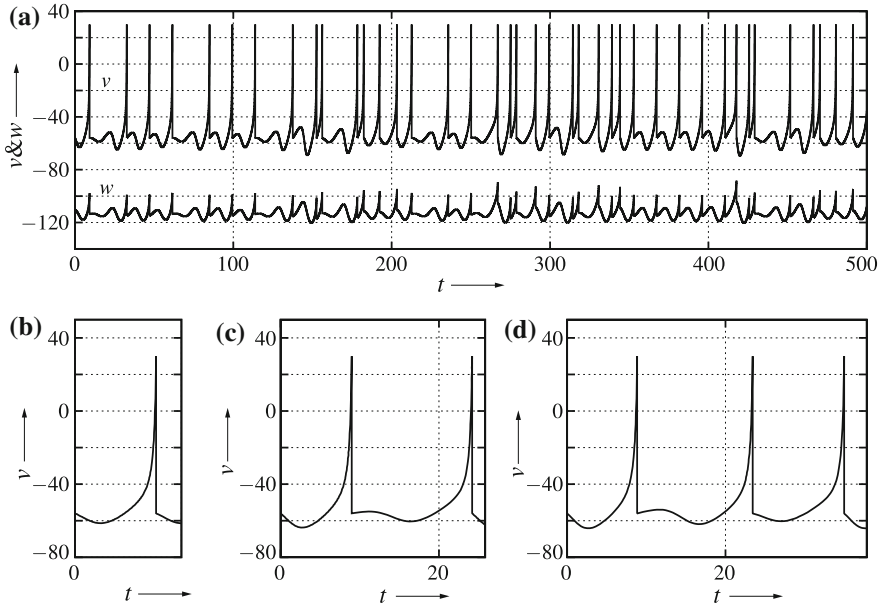

Fig. 6.13 Phase portraits of a chaotic attractor and UPOs by the numerical simulation, where $a = 0.2$, $b = 2$, $c = -56$, $d = -16$, $I = -99$, and $\theta = 30$. These UPOs are embedded in the chaotic attractor

6.4.1 Controller

The stabilizing control is applied to UPOs in Table 6.2. The Poincaré section is defined as: $\Pi = \left\{z \in \mathbb{R}^2 |\, q(z) = v - \theta = 0\right\}$.

Table 6.2 Periods, states, and multipliers of UPOs in Fig. 6.13

Attractor	Period	w^* ($v^* = c = 56$)	μ
UPO_1	1	−111.734371227672	−2.192843924301
UPO_2	2	−114.280257572631	−9.910331534347
		−109.950121533113	
UPO_3	3	−114.603487249294	+25.322864600880
		−112.427919143969	
		−109.602553091223	

From (6.8) and (6.9), the control gain is computed as follows:

$$K = \frac{q - D_{w^*}}{D_\theta},$$

where $D_{w^*} = \partial T/\partial w^*$ and $D_\theta = \partial T/\partial \theta$. The derivatives of the Poincaré map are obtained by (6.3) and (6.4). Now q is a desirable pole for the controller, and $|q| < 1$ is required for stabilization. The control input $u(k)$ is generated by the gain $K \in \mathbb{R}$ and the state $z(t)$ as $K(w^* - w(\tau))$ from (6.7). It is renewed after the jumping dynamics, and added to the threshold value θ as a perturbation. Since θ is only referred as the threshold value of the jumping dynamics, $u(k)$ does not affect the dynamical equations during the transition state.

6.4.2 Numerical Simulation

We show some results of the chaos control in Fig. 6.14, where each diagram shows a transition response of the orbit and the threshold value with the controlling signal. From these figures, we confirmed that each UPO has been controlled to become a stable periodic orbit by several renewals of $u(t)$. To prevent generating big amplitude of the control, a limiter is provided in the controller. The condition is given as follows:

$$\text{if} \quad |u(t)| \geq 20 \quad \text{then} \quad u(t) \leftarrow 0.$$

Figure 6.15 shows the basins of attraction of UPOs with our controller in the q-$w(0)$ plane. White regions in Fig. 6.15 indicate the initial values in which the UPO can be stabilized, and black regions indicate failure of the controlling.

Figure 6.13 reveals that the chaotic attractor wanders within $-125 < w < -100$ on the Poincaré section. The basin of attraction in this range is shown by the white regions in Fig. 6.15. Thus UPOs are stabilized robustly, and the threshold control for the piecewise nonlinear system performs well.

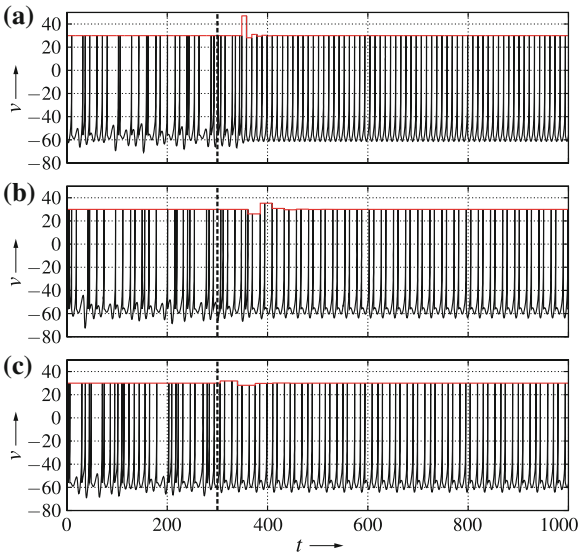

Fig. 6.14 Transition responses of controlled UPOs and the threshold values. **a** Period-1, **b** period-2 and **c** period-3 solutions shown in Table 6.2 are stabilized, and the final threshold value is 30 [mV]. Note that $u(t)$ is not applied to the system as a continuous input, but only updates the threshold value

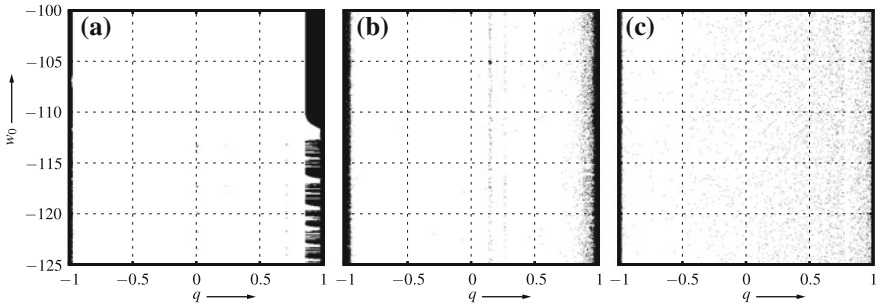

Fig. 6.15 Basins of attraction resulting from a control experiment. (*White* stabilizable regions and *black* unstabilizable regions.) The *horizontal* and *vertical axes* are the parameter q of the controller and the initial state of the system, respectively

6.5 Conclusion

We have proposed a control method for UPOs embedded in hybrid chaotic systems by variable threshold values. First, we have explained how to design the controlling gain of assigning poles with the perturbation of a switching threshold value. The pole assignment method requires the derivatives of the Poincaré map about threshold values, for which we have proposed the technique to calculate. We have also

demonstrated the design of a controller and numerical simulations of the controlling for a 1D switching chaotic system and a 2D chaotic neuron model. Some simulation results indicate that our controller stabilizes target UPOs well. Additionally, we have implemented our controller in a real circuit and presented experimental results. From them, it is confirmed that our controller can be implemented in a real circuit, and also well performed without technical difficulties.

For modeling biological and medical systems, the hybrid dynamical systems are widely used [27]. For example, Akakura et al. [28] reported that the intermittent hormone therapy could be effective in the hormone treatment of prostate cancer. This therapy switches the treatment on and off based on the observation of the serum prostate-specific antigen (PSA) level. Therefore, the therapy can be represented as a hybrid dynamical system, and some PSA levels are defined as the switching threshold values. The mathematical modeling of the intermittent hormone therapy has been investigated intensively [29]. Since our method is available for general piecewise nonlinear systems and the threshold perturbation seems to be related to the intermittent hormone therapy, it is worth investigating a possibility whether our method is applicable for the prostate cancer treatment or not.

Acknowledgments The authors wish to thank International Journal of Bifurcation and Chaos, World Scientific Publishing for granting permission to present here a modified version of the material published in "Controlling chaos of hybrid systems by variable threshold values," D. Ito, T. Ueta, T. Kousaka, J. Imura, and K. Aihara, International Journal of Bifurcation and Chaos, Vol. 24, No. 10, http://www.worldscientific.com/doi/abs/10.1142/S0218127414501259 ©2014 World Scientific Publishing Company [30].

References

1. Auerbach, D., Cvitanović, P., Eckmann, J.-P., Gunaratne, G.: Exploring chaotic motion through periodic orbits. Phys. Rev. Lett. **23**, 2387–2389 (1987)
2. Ott, E., Grebogi, C., Yorke, J.A.: Controlling chaos. Phys. Rev. Lett. **64**, 1196–1999 (1990)
3. Romeiras, F.J., Grebogi, C., Ott, E., Dayawansa, W.P.: Controlling chaotic dynamical systems. Physica D **58**(1–4), 165–192 (1992)
4. Kousaka, T., Ueta, T., Kawakami, H.: Controlling chaos in a state-dependent nonlinear system. Int. J. Bifurcat. Chaos **12**(5), 1111–1119 (2002)
5. Ueta, T., Kawakami, H.: Composite dynamical system for controlling chaos. IEICE Trans. Fundam **E78-A**(6), 708–714 (1995)
6. Kousaka, T., Ueta, T., Ma, Y., Kawakami, H.: Control of chaos in a piecewise smooth nonlinear system. Chaos, Solitons Fractals **27**(4), 1019–1025 (2006)
7. Pyragas, K.: Delayed feedback control of chaos. Phil. Trans. R. Soc. A **15**, **364**(1846), 2309–2334 (2006)
8. Perc, M., Marhl, M.: Detecting and controlling unstable periodic orbits that are not part of a chaotic attractor. Phys. Rev. E **70**, 016204 (2004)
9. Perc, M., Marhl, M.: Chaos in temporarily destabilized regular systems with the slow passage effect. Chaos, Solitons Fractals **7**(2), 395–403 (2006)
10. Pyragas, K.: Continuous control of chaos by self-controlling feedback. Phys. Lett. A **70**(6), 421–428 (1992)
11. Myneni, K., Barr, T.A., Corron, N.J., Pethel, S.D.: New method for the control of fast chaotic oscillations. Phys. Rev. Lett. **83**, 2175–2178 (1999)

12. Rajasekar, S., Lakshmanan, M.: Algorithms for controlling chaotic motion: application for the BVP oscillator. Physica D **67**(1–3), 282–300 (1993)
13. Roy, R., Murphy, T.W., Maier, T.D., Gills, Z., Hunt, E.R.: Dynamical control of a chaotic laser: Experimental stabilization of a globally coupled system. Phys. Rev. Lett. **68**, 1259–1262 (1992)
14. Sabuco, J., Zambrano, S., Sanjuán, M.A.F.: Partial control of chaotic transients using escape times. New J. Phys. **12**, 113038 (2010)
15. Starrett, J.: Control of chaos by occasional bang-bang. Phys. Rev. E **67**, 036203 (2003)
16. Zambrano, S., Sanjuán, M.A.F.: Exploring partial control of chaotic systems. Phys. Rev. E **79**, 026217 (2009)
17. Leine, R., Nijmeijer, H.: Dynamics and Bifurcations of Non-smooth Mechanical Systems. Springer, Berlin (2004)
18. Bernardo, M., Budd, C.J., Champneys, A.R., Kowalczyk., P.: Piecewise-Smooth Dynamical Systems: Theory and Applications. Springer, London (2008)
19. Inagaki, T., Saito, T.: Consistency in a chaotic spiking oscillator. IEICE Trans. Fundam. **E91-A**(8), 2040–2043 (2008)
20. Ito, D., Ueta, T., Aihara, K.: Bifurcation analysis of two coupled Izhikevich oscillators. Proc. IEICE/NOLTA2010, 627–630 (2010)
21. Kousaka, T., Ueta, T., Kawakami, H.: Bifurcation of switched nonlinear dynamical systems. IEEE Trans. Circ. Syst. **CAS-46**(7), 878–885 (1999)
22. Murali, K., Sinha, S.: Experimental realization of chaos control by thresholding. Phys. Rev. E **68**, 016210 (2003)
23. Kousaka, T., Tahara, S., Ueta, T., Abe, M., Kawakami, H.: Chaos in simple hybrid system and its control. Electron. Lett. **37**(1), 1–2 (2001)
24. Kousaka, T., Kido, T., Ueta, T., Kawakami, H., Abe, M.: Analysis of border-collision bifurcation in a simple circuit. Proc. IEEE/ISCAS **2**, 481–484 (2000)
25. Izhikevich, E.M.: Simple model of spiking neurons. IEEE Trans. Neural Netw. **14**(6), 1569–1572 (2003)
26. Tamura, A., Ueta, T., Tsuji, S.: Bifurcation analysis of Izhikevich neuron model. Dyn. Continuous, Discrete Impulsive Syst. **16**(6), 849–862 (2009)
27. Aihara, K., Suzuki, H.: (2010) Theory of hybrid dynamical systems and its applications to biological and medical systems. Phil. Trans. R. Soc. A. **13**(368), 4893–4914 (1930)
28. Akakura, K., Bruchovsky, N., Goldenberg, S.L., Rennie, P.S., Buckley, A.R., Sullivan, L.D.: Effects of intermittent androgen suppression on androgen-dependent tumors. Apoptosis and serum prostate-specific antigen. Cancer **71**, 2782–2790 (1993)
29. Tanaka, G., Hirata, Y., Goldenberg, S.L., Bruchovsky, N., Aihara, K.: Mathematical modelling of prostate cancer growth and its application to hormone therapy. Phil. Trans. R. Soc. A. **13**, **368**(1930), 5029–5044 (2010)
30. Ito, D., Ueta, T., Kousaka, T., Imura, J., Aihara, K.: Controlling chaos of hybrid systems by variable threshold values. Int. J. Bifurcat. Chaos **24**(10), 1450125 (2014) (12 pages)